THE JOURNAL OF BIOLOGICAL CHEMISTRY VOL. 285, NO. 51, pp. 39866–39875, December 17, 2010

Dioxygenase Activity of Epidermal Lipoxygenase-3 Unveiled

TYPICAL AND ATYPICAL FEATURES OF ITS CATALYTIC ACTIVITY WITH NATURAL AND SYNTHETIC POLYUNSATURATED FATTY ACIDS[*][S]

Received for publication, June 16, 2010, and in revised form, September 30, 2010 Published, JBC Papers in Press, October 4, 2010, DOI 10.1074/jbc.M110.155374

Yuxiang Zheng and Alan R. Brash[1]

From the Department of Pharmacology and the Vanderbilt Institute of Chemical Biology, Vanderbilt University School of Medicine, Nashville, Tennessee 37232

Epidermal lipoxygenase-3 (eLOX3) exhibits hydroperoxide isomerase activity implicated in epidermal barrier formation, but its potential dioxygenase activity has remained elusive. We identified herein a synthetic fatty acid, 9*E*,11*Z*,14*Z*-20:3ω6, that was oxygenated by eLOX3 specifically to the 9*S*-hydroperoxide. Reaction showed a pronounced lag phase, which suggested that eLOX3 is deficient in its activation step. Indeed, we found that high concentrations of hydroperoxide activator (*e.g.* 65 μM) overcame a prolonged lag phase (>1 h) and unveiled a dioxygenase activity with arachidonic acid; the main products were the 5-, 9-, and 7-hydroperoxyeicosatetraenoic acids (HPETEs). These were *R*/*S* mixtures (ranging from ~50:50 to 73:27), and as the bis-allylic 7-HPETE can be formed only inside the enzyme active site, the results indicate there is oxygen availability along either face of the reacting fatty acid radical. That the active site oxygen supply is limited is implied from the need for continuous re-activation, as carbon radical leakage leaves the enzyme in the unactivated ferrous state. An Ala-to-Gly mutation, known to affect the positioning of O_2 in the active site of other lipoxygenase enzymes, led to more readily activated reaction and a significant increase in the 9*R*- over the 5-HPETE. Activation and cycling of the ferric enzyme are thus promoted using the 9*E*,11*Z*,14*Z*-20:3ω6 substrate, by continuous hydroperoxide activation, or by the Ala-to-Gly mutation. We suggest that eLOX3 represents one end of a spectrum among lipoxygenases where activation is inefficient, favoring hydroperoxide isomerase cycling, with the opposite end represented by readily activated enzymes in which dioxygenase activity is prominent.

Epidermal lipoxygenase-3 (eLOX3)[2] is one of the two lipoxygenases (LOX) involved in skin barrier formation (1, 2). Inactivating mutations in either the gene encoding human eLOX3 or the gene encoding 12*R*-LOX lead to impaired skin barrier function that manifests itself in the disease autosomal recessive congenital ichthyosis (3, 4). The scaly skin phenotype of this disease is a compensatory response to the fundamental defect in the barrier function (5). Targeted gene knockouts or ethylnitrourea mutagenesis in mice confirm the role of these two LOX enzymes, and in both cases the mice die soon after birth due to severe transepidermal water loss (6–8).

In addition to its involvement in skin barrier formation, eLOX3 also attracts attention because of its unusual enzymology. It is classified as a LOX based on its amino acid sequence (*e.g.* 58% identity to 12*R*-LOX) yet its name eLOX3 lacks the usual designation such as 5-, 12-, or 15-LOX. The reason is the enzyme appears to be devoid of typical dioxygenase activity with polyunsaturated fatty acid substrates such as arachidonic acid (9, 10). Instead, it displays a novel hydroperoxide isomerase activity that efficiently converts fatty acid hydroperoxides, the usual LOX products, to epoxyalcohols and ketones (10). This hydroperoxide isomerase activity, acting on a hydroperoxide product of 12*R*-LOX, has been proposed to be the physiological function of eLOX3 (1).

The non-heme iron in the active site of LOX enzymes exists in two oxidation states, ferrous and ferric. Native LOX are usually in the ferrous state, yet only the ferric enzyme is catalytically active as a dioxygenase (11). Therefore, to enter the catalytic cycle the ferrous enzyme has to be oxidized to the ferric form first, usually by 1 eq of their own hydroperoxide product. This process, commonly known as the activation step, accounts for the initial lag phase in the progress curve of LOX reactions (12, 13). Because the reaction between typical LOX and fatty acid hydroperoxides is only a single turnover event, no significant products would accumulate unless an iron-reducing agent such as nordihydroguaiaretic acid (NDGA) is given to regenerate the ferrous enzyme (14) (Fig. 1*A*).

Unlike typical LOX, eLOX3 does not require iron-reducing agents for its hydroperoxide isomerase activity. That this reaction is catalysis, rather than a single turnover, implies that the ferrous state of eLOX3 is largely preserved. However, NDGA does speed up the reaction (10), suggesting that the enzyme can be oxidized by fatty acid hydroperoxides to some extent. We reasoned that the activation step of the LOX activity in eLOX3, if it does occur, would be very inefficient, requiring many molecules of fatty acid hydroperoxide to oxidize one molecule of eLOX3 (Fig. 1*B*). In other words, higher than usual concentrations of fatty acid hydroperoxide might be

* This work was supported, in whole or in part, by National Institutes of Health Grant AR-051968 (to A. R. B.).

[S] The on-line version of this article (available at http://www.jbc.org) contains supplemental Figs. S1–S4 and an additional reference.

[1] To whom correspondence should be addressed: Dept. of Pharmacology, Vanderbilt University School of Medicine, 23rd Ave. S at Pierce, Nashville, TN 37232-6602. Tel.: 615-343-4495; Fax: 615-322-4707; E-mail: alan.brash@vanderbilt.edu.

[2] The abbreviations used are: eLOX3, epidermal lipoxygenase-3; H(P)ETE, hydro(pero)xyeicosatetraenoic acid; AA/lyso-PA, arachidonoyl-lysophosphatidic acid; NDGA, nordihydroguaiaretic acid; LOX, lipoxygenase; SP-HPLC, straight phase-HPLC; RP-HPLC, reversed phase-HPLC; 4-hydroxy-TEMPO, 4-hydroxy-2,2,6,6-tetramethylpiperidine 1-oxyl; TMS, trimethylsilyl.

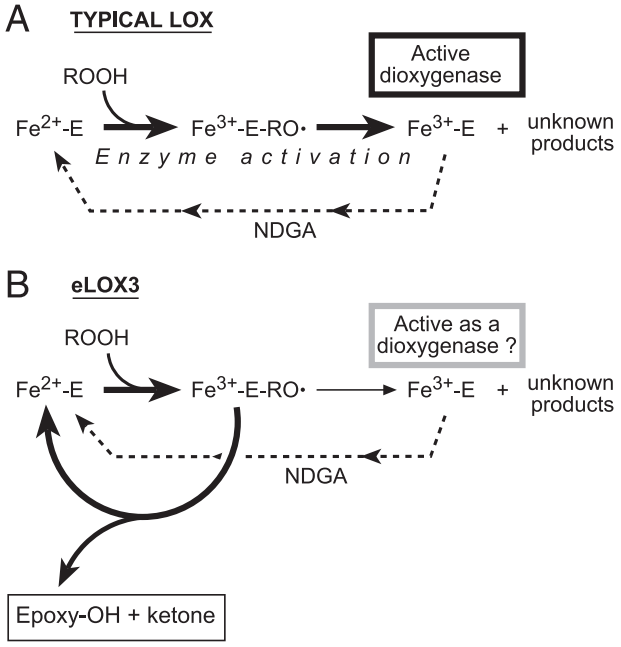

FIGURE 1. **Comparison of typical LOX and eLOX3 reactions with fatty acid hydroperoxide (ROOH).** *A,* for typical LOX, 1 eq of ROOH oxidizes the Fe(II) enzyme to the Fe(III) form, via the Fe(III) enzyme-alkoxyl radical (RO•) intermediate. NDGA reduces the Fe(III) enzyme back to Fe(II) and thus inhibits its dioxygenase activity. *B,* for eLOX3, more than 1 eq of ROOH is required to oxidize the Fe(II) enzyme, because the Fe(III) enzyme-RO• intermediate usually undergoes hydroperoxide isomerase cycling with formation of epoxyalcohols and ketones. Occasionally, the Fe(III) enzyme-RO• intermediate converts to the free Fe(III) enzyme. NDGA reduces the Fe(III) enzyme and thus stimulates hydroperoxide isomerase activity.

required to activate eLOX3. This inefficiency in the activation step of eLOX3 could potentially account for its apparent lack of dioxygenase activity, which must be performed by the activated ferric enzyme.

An additional explanation for the lack of dioxygenase activity in eLOX3 might be that the active site iron has a low redox potential. This redox requirement is imposed by the first chemical step of the dioxygenase cycle, which involves homolytic cleavage of a bis-allylic C–H bond in the fatty acid substrate by the active site Fe(III)-OH complex (15). The moderately high bond dissociation energy of this C–H bond (*e.g.* ~73 kcal/mol for C_7-H, C_{10}-H, or C_{13}-H in arachidonic acid (16)) dictates that the redox potential of the active site iron should also be moderately high for the bond cleavage to occur (17). Indeed, a moderately high redox potential of ~600 mV has been demonstrated experimentally in the prototypical LOX, soybean LOX-1 (18). Unfortunately, a direct test of this hypothesis, by measuring the redox potential of eLOX3 for comparison with soybean LOX-1, is not yet possible due to difficulties in preparing multiple milligrams of purified eLOX3 for EPR spectroscopy.

In this study, we set out to test indirectly the redox potential hypothesis by incubating eLOX3 with a panel of synthetic fatty acids with extended conjugation. Because of the extended conjugation, these fatty acids are easier to oxidize than typical polyunsaturated fatty acids such as arachidonic acid (16) and thus might be accepted by eLOX3 as substrate. The study on this panel of synthetic fatty acids revealed some unusual characteristics of eLOX3 that prompted us to consider the other possibility that eLOX3 does not react with natural fatty acids because it is deficient in the activation step. To further test this possibility, we reexamined the reaction eLOX3 with arachidonic acid using high concentrations of hydroperoxide activator. We also studied the effect of an Ala-to-Gly mutation in the active site that is known to affect oxygenation specificity (19, 20), and we investigated the effect of substrate orientation on product specificity using the large ester arachidonoyl-lysophosphatidic acid (AA/lyso-PA). "Discussion" ties the findings together and proposes a model with mechanistic relevance to the understanding of LOX enzymes in general.

EXPERIMENTAL PROCEDURES

Materials—Arachidonic and linoleic acids were purchased from NuChek Prep Inc. (Elysian, MN). 15*S*-HPETE or 13*S*-HPODE was synthesized by reacting soybean LOX-1 with arachidonic acid or linoleic acid at pH 9 followed by SP-HPLC purification (21). 12*R*-HPETE was synthesized by autoxidation (10). 4-Hydroxy-TEMPO was purchased from Sigma, and AA/lyso-PA was purchased from Avanti Polar Lipids, Inc. (Alabaster, AL).

Chemical Synthesis of Conjugated Fatty Acids—9*E*,11*Z*,14*Z*-20:3ω6 was synthesized by Dr. Jin K. Cha, Wayne State University, as described previously (22). 8*Z*,11*Z*,13*E*-20:3ω7 was a kind gift from Dr. K. C. Nicolaou at the Scripps Research Institute. 11*Z*,14*Z*,16*E*-20:3ω4 and 12*E*,14*Z*,17*Z*-20:3ω3 were synthesized by alkaline isomerization (23) of 11*Z*,14*Z*,17*Z*-20:3ω3 (NuChek Prep Inc., Elysian, MN) and 9*Z*,12*Z*,14*E*-18:3ω4 by alkaline isomerization of α-linolenic acid (NuChek Prep Inc., Elysian, MN)). Briefly, 10 mg of the precursor fatty acid was dissolved in 1 ml of 1 N KOH in ethylene glycol, flushed with argon, and placed in an oven at 144 °C. The extent of the reaction was monitored every 10 min by UV spectrophotometry assay of an aliquot, and the reaction was stopped when UV absorbance at 235 nm ceased to increase (total reaction time was about 20–30 min). The reaction mixture was then acidified by 1 N HCl to pH 3 and extracted by methylene chloride. The extract was analyzed by silver ion chromatography, and the two desired products were identified based on their UV (identical to that of 9*E*,11*Z*,14*Z*-20:3ω6) and ^{1}H and ^{1}H,^{1}H-COSY NMR spectra.

Expression and Purification of Human eLOX3—The cDNA of human eLOX3 with an N-terminal His tag was subcloned into the pCW vector, and the protein was expressed and purified according to a previously published protocol (24). Flat-bottomed 500-ml flasks, which were found to give a higher yield of eLOX3 than baffled flasks, were used for the 50-ml cultures.

Reaction Incubations—The room temperature reaction with 9*E*,11*Z*,14*Z*-20:3ω6 was monitored by UV spectrophotometry. By contrast, 0 °C reactions and the room temperature reaction with arachidonic acid were not monitored by UV spectroscopy. For the latter, incubation was typically conducted in a 5-ml reactivial. First, the fatty acid substrate and the auxiliary components to be investigated (*e.g.* hydroperoxide activators, 4-hydroxy-TEMPO) were added to an empty vial and then taken to dryness under a stream of N_2. Next, 2

ml of 100 mM sodium phosphate buffer, pH 7.5, was added, and the vial was capped and subjected to vortex. Next, the enzyme was added to start the reaction. Finally, the reaction was quenched by addition of methanol (usually 1 ml). For time course experiments with arachidonic acid, at specified time points, an aliquot (usually 150–200 μl) of the incubation mixture was taken out and immediately added to a separate vial containing 833 ng of 9*E*,11*Z*,14*Z*-20:3ω6, the internal standard, in 0.5 ml of methanol. The 0 °C reaction with AA/lyso-PA was performed under the same conditions as the 0 °C reaction with arachidonic acid. The lysophospholipid was chosen for this study because of its better solubility in aqueous solutions than those of diacyl phospholipids (25).

Extraction of Reaction Products—The incubation mixture was acidified to pH 5 using 1 N HCl, treated with more than 1 M eq of $SnCl_2$ on ice for 10 min, and then extracted by an Oasis HLB cartridge (Waters Corp.).

HPLC Analysis—For reaction with 9*E*,11*Z*,14*Z*-20:3ω6, SP HPLC analysis used a Beckman silica column (0.46 × 25 cm), a solvent system of hexane/isopropyl alcohol/acetic acid (100:1.5:0.1, by volume), and a flow rate of 1 ml/min. Chiral phase HPLC analysis used a Daicel ChiralPak AD column (0.46 × 25 cm), a solvent system of hexane/ethanol/acetic acid (100:5:0.05), and a flow rate of 1 ml/min.

For reaction with arachidonic acid, RP-HPLC analysis of HETE products was performed using a Waters Symmetry C18 column (0.46 × 25 cm), a solvent system of methanol/water/acetic acid (80:20:0.01), and a flow rate of 1 ml/min. For time course experiments, RP-HPLC analysis used the same column, methanol/water/acetic acid (95:5:0.01), and 1 ml/min. The remaining arachidonic acid substrate and accumulated 9- and 5-HPETE products in the time course experiments were quantified by comparison of their corresponding peak area with that of the internal standard, 9*E*,11*Z*,14*Z*-20:3ω6. To avoid rearrangement of bis-allylic HETEs, which may occur under even mildly acidic conditions (26), HPLC analyses with no acid-containing solvent systems were also performed on reaction extract pretreated with ethereal diazomethane, which converts free acids to methyl esters. 7-HETE and 11-HETE methyl esters were separated using a Beckman silica column (0.46 × 25 cm), an isocratic solvent system of hexane/isopropyl alcohol (100:2, by volume), and a flow rate of 1 ml/min. The relative abundance of each HETE product was estimated based on the 205 nm absorbance. (This is justified by a previous study showing that the radioactive trace of [1-^{14}C]HETEs matches well with the corresponding UV trace at 205 nm (26).) Chiral analysis used a Daicel ChiralPak AD column (0.46 × 25 cm), isocratic solvent of hexane/methanol (100:1.5), and a flow rate of 1 ml/min. The stereo-configuration of methyl 7-HETE enantiomers on chiral HPLC was deduced based on the finding that bis-allylic HETEs would undergo mainly "suprafacial" rearrangement upon mild acid treatment (26). Briefly, the two enantiomers (1–2 μg) were purified by chiral HPLC, repeatedly (4–5 cycles) treated with 1 ml of methanol/water/acetic acid (75:25:1) followed by evaporation under N_2, and then subjected to chiral HPLC analysis. For example, the second peak of 7-HETE methyl ester on chiral HPLC was found to rearrange mainly to 5*S*-HETE and 9*R*-HETE methyl esters and was thus deduced to be 7*R*, because 7*R*-hydroxyl sits on the same face of the double bond system in the fully extended configuration as does the 5*S*- or 9*R*-hydroxyl.

For reaction with AA/lyso-PA, the products were transmethylated after extraction using a previously published protocol (27), followed by RP-HPLC analysis using a Waters Symmetry C18 column (0.46 × 25 cm), an isocratic solvent system of methanol/water (80/20), and a flow rate of 1 ml/min.

Derivatization and GC-MS Analysis—Catalytic hydrogenations were performed in 100 μl of ethanol using about 1 mg of palladium on alumina and bubbling with hydrogen for 2 min at room temperature. The hydrogenated products were recovered by the addition of water and extraction with ethyl acetate. Trimethylsilyl (TMS) ether derivatives were prepared by treatment with bis(trimethylsilyl)-trifluoroacetamide (10 μl) and pyridine (2 μl) at room temperature for 2 h. Subsequently, the reagents were evaporated under a stream of nitrogen, and the samples were dissolved in hexane for GC-MS.

Analysis of the methyl ester trimethylsilyl ether derivatives of the products was carried out in the positive ion electron impact mode (70 eV) using a Thermo Finnigan Trace DSQ ion trap GC-MS with the Xcalibur data system. Samples were injected at 150 °C, and after 1 min the temperature was programmed to 300 °C at 20 °C/min. The spectra shown under Results were averaged from about 10 spectra collected during elution of the GC peaks.

RESULTS

Dioxygenase Activity of eLOX3 with 9E,11Z,14Z-20:3ω6—To examine the potential oxygenase activity of eLOX3, we tested eLOX3 with a series of synthetic fatty acids with extended conjugation (their structures are shown in supplemental Fig. S1). Among these fatty acids, only 9*E*,11*Z*,14*Z*-20:3ω6 turned out to be a good substrate. The initial reactions of eLOX3 (0.1 μM) with 9*E*,11*Z*,14*Z*-20:3ω6 (18 μM) were conducted at room temperature and monitored by scanning UV spectrophotometry. The substrate contains a conjugated diene chromophore and absorbs strongly at 235 nm (Fig. 2*A*, *dotted line*). Upon addition of enzyme, the UV absorbance of the substrate gradually decreased, whereas a new chromophore typical of conjugated trienes came to prominence (λ_{max} ~270 nm; Fig. 2*A*). Monitoring of the rate of reaction at 235 nm revealed a pronounced lag phase of ~5 min during which time no significant reaction is apparent (Fig. 2*B*); addition of exogenous hydroperoxide activator (1 μM 13*S*-HPODE) almost eliminated the lag phase. Kinetic measurements of initial rates over a range of substrate concentrations gave estimates of K_m and k_{cat} as 50 μM and 1.6 s^{-1}, respectively (Fig. 2*C*).

Products of the 9E,11Z,14Z-20:3ω6 Reaction at Room Temperature—SP and RP-HPLC analyses revealed a complex product pattern, including at least four products with λ_{max} at 270 nm, four at 235 nm, and four at 320 nm (data not shown). We reasoned that the substrate was first oxygenated to conjugated triene hydroperoxides (λ_{max} 270 nm), which were then further converted by the hydroperoxide isomerase activity of

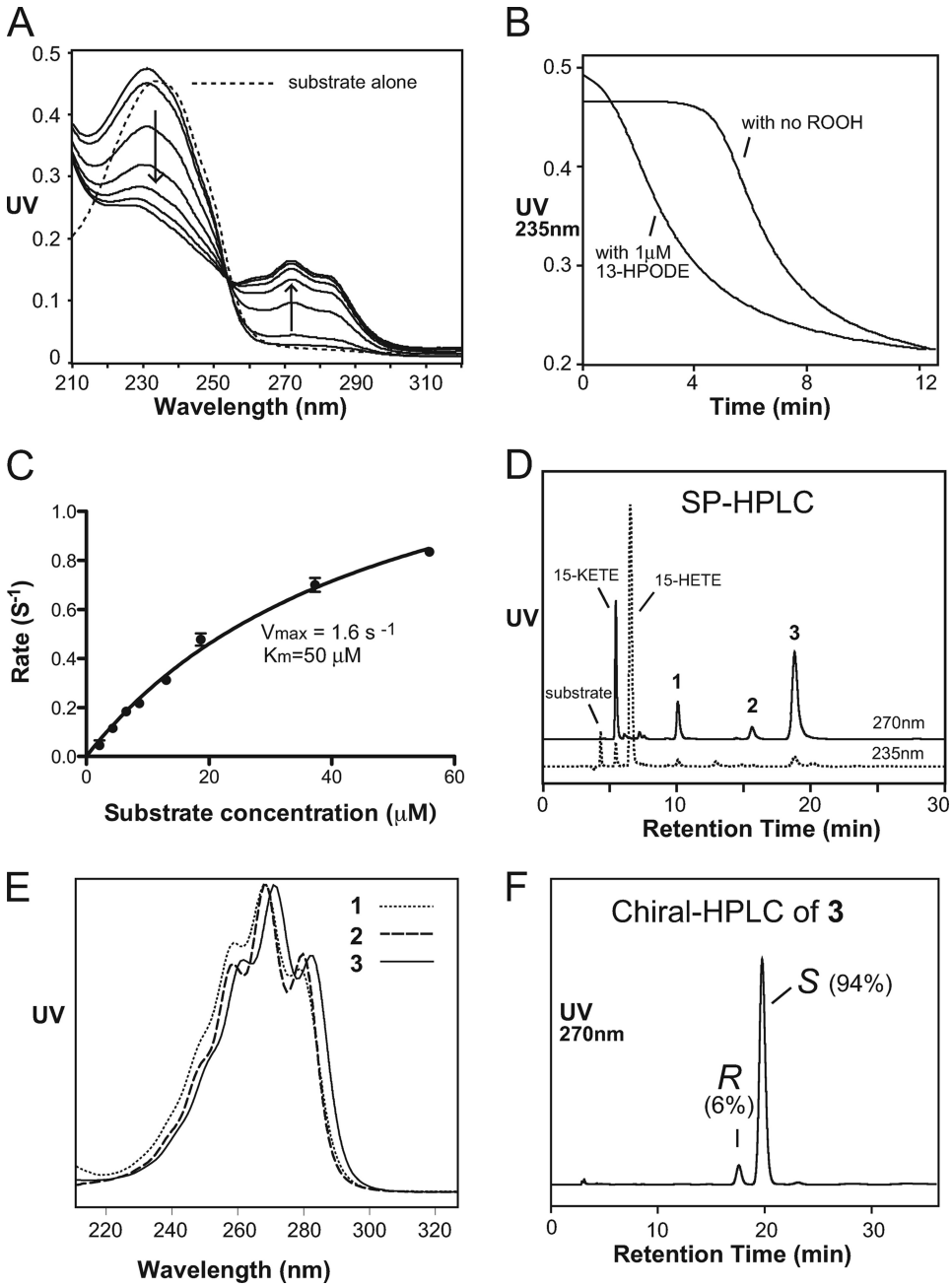

FIGURE 2. **Dioxygenase activity of eLOX3 with 9*E*,11*Z*,14*Z*-20:3ω6.** *A*, UV scans of the room temperature reaction of eLOX3 (0.1 μM) with 9*E*,11*Z*,14*Z*-20:3ω6 (18 μM). To 1 ml of phosphate buffer, pH 7.5, the substrate was added, and a UV scan was taken (*dotted line*). After the enzyme was added and mixed (for ~15 s), a second scan was taken. Further scans shown were taken after 3–8 min. *B*, progress curves of the reaction in the absence or presence of 13*S*-HPODE, monitored at 235 nm. The reaction conditions are the same as in *A*. *C*, dependence of maximal rate on substrate concentration. Maximal rates were taken from the steepest part of progress curves. *D*, straight phase (*SP*)-HPLC analysis of the primary products. Here, the reaction of eLOX3 (0.13 μM) with 9*E*,11*Z*,14*Z*-20:3ω6 (33 μM) was performed at 0 °C, in the presence of 15*S*-HPETE (150 μM) and 4-hydroxy-TEMPO (1.5 mM). The reaction was completed within 30 min. *E*, UV spectra (in straight phase solvent) of products **1–3**, as designated in *D*. *F*, Chiral HPLC analysis of product **3**.

eLOX3 to epoxyalcohols and ketones (λ_{max} 235 and 320 nm; for postulated structures, see supplemental Fig. S2). The fact that the epoxyalcohol products also absorb at 235 nm explains why a substantial UV absorbance at 235 nm remained upon completion of the reaction (Fig. 2*A*).

Trapping of the Primary Products—To focus on the primary LOX reaction, we identified the following three key factors that almost eliminated secondary product formation: (i) incubation at 0 °C preferentially reduces hydroperoxide isomerase activity compared with dioxygenase activity (28–31); (ii) an excess of 15*S*-HPETE included in the incubation competes with the conjugated triene hydroperoxide products for the hydroperoxide isomerase activity, and the excess 15*S*-HPETE helps keep the enzyme in the ferric state (see below); and (iii), addition of 4-hydroxy-TEMPO (1.5 mM), a water-soluble antioxidant, prevents nonenzymatic lipid peroxidation without causing significant enzyme inhibition (32). At the end of the incubation, $SnCl_2$ was added to convert hydroperoxides to the more stable alcohols, and the products were extracted and analyzed by SP-HPLC with a diode-array detector (Fig. 2, *D*

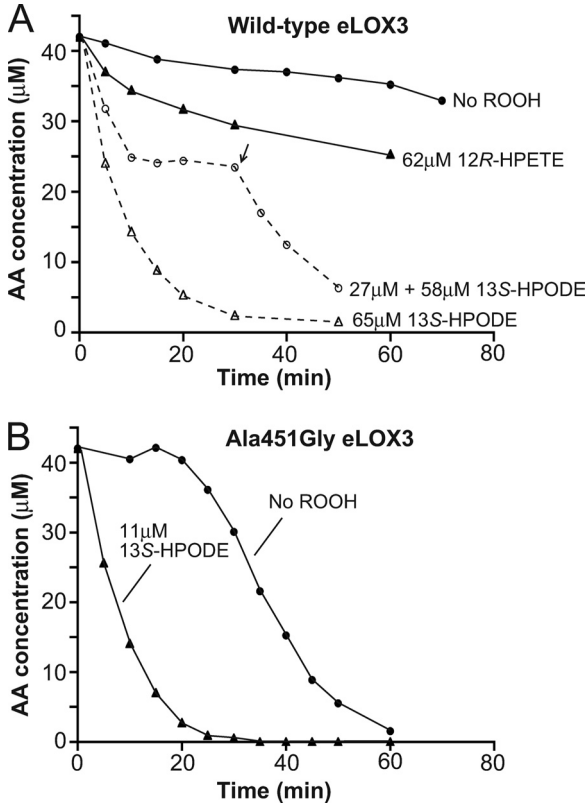

FIGURE 3. **Effect of fatty acid hydroperoxide on dioxygenase activity of wild-type eLOX3 (0.4 μM) (*A*) or A451G eLOX3 (0.5 μM) (*B*) with arachidonic acid (42 μM) at room temperature.** Arachidonic acid (**AA**) and fatty acid hydroperoxides were added first to phosphate buffer, pH 7.5, and then addition of enzyme started the reactions. At specified time points, an aliquot was taken, and the unreacted arachidonic acid substrate was quantified by RP-HPLC. *Arrow* in *panel A*, a second aliquot of 13*S*-HPODE (58 μM) was added at 30 min.

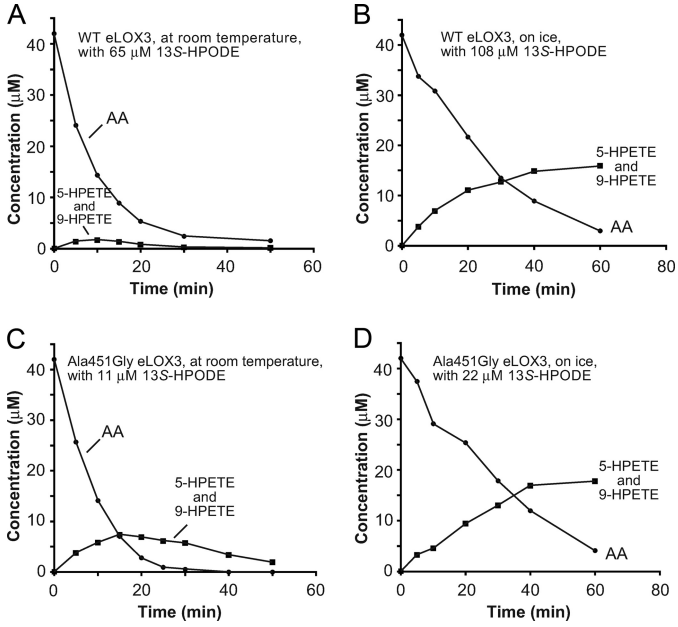

FIGURE 4. **Effect of temperature on accumulation of HPETE products in the reaction of wild-type eLOX3 (0. 4 μM) or A451G eLOX3 (0.5 μM) with arachidonic acid (*AA*) (42 μM).** 5-HPETE and 9-HPETE shown on the plots represented over 50% of the total products and could be readily quantified by RP-HPLC analysis. *A,* wild-type eLOX3 reaction at room temperature in the presence of 65 μM 13*S*-HPODE. *B,* wild-type eLOX3 reaction at 0 °C in the presence of 108 μM 13*S*-HPODE. *C,* A451G eLOX3 reaction at room temperature in the presence of 11 μM 13*S*-HPODE. *D,* A451G eLOX3 reaction at 0 °C in the presence of 22 μM 13*S*-HPODE.

and *E*). By comparison with authentic standards obtained in a previous study (22) and by GC-MS analysis, the major peak **3** (76%) was identified as 9-hydroxy-10*E*,12*E*,14*Z*-eicosatrienoic acid, and the two minor products **1** and **2** as positional and geometric isomers of **3**. (Products **1** and **2** both have a 15-hydroxyl but differ in double bond configuration; data not shown). Chiral phase HPLC resolved product **3** into the *R* and *S* isomers with a ratio of 6:94 (Fig. 2*F*). Thus, 9*E*,11*Z*,14*Z*-20:3ω6 was oxygenated by eLOX3 in a regio- and stereospecific fashion to its 9*S*-hydroperoxy derivative, 9*S*-hydroperoxy-10*E*,12*E*,14*Z*-eicosatrienoic acid. The 9*S*-oxygenation occurs four carbons removed from the site of hydrogen abstraction at C-13. None of the other conjugated fatty acids tested were significantly oxygenated, indicating substrate selectivity of eLOX3.

Dioxygenase Activity of eLOX3 with Arachidonic Acid—The pronounced lag phase seen with 9*E*,11*Z*,14*Z*-20:3ω6 led us to question whether there might be an even longer lag phase with arachidonic acid, which might be overcome using fatty acid hydroperoxide activator. As shown in Fig. 3*A*, in the absence of fatty acid hydroperoxides, eLOX3 (0.4 μM) showed only weak and slow activity with arachidonic acid (42 μM) as monitored by RP-HPLC assay of the remaining substrate. In the presence of high concentrations of fatty acid hydroperoxides, however, the rate of conversion of arachidonic acid was greatly accelerated, more so in the presence of 13*S*-HPODE than in the presence of 12*R*-HPETE. Also, the effect of fatty acid hydroperoxides is dose-dependent, as 65 μM 13*S*-HPODE proved to be more effective than 27 μM 13*S*-HPODE. In fact, the reaction initiated with 27 μM 13*S*-HPODE was found to stall when 13*S*-HPODE was fully consumed and to resume only after a second dose of 13*S*-HPODE (58 μM) was given. Therefore, the reaction of eLOX3 with arachidonic acid coincided with and was likely driven by its reaction with fatty acid hydroperoxides.

Dioxygenase Activity of A451G eLOX3 with Arachidonic Acid—The stereospecificity of oxygenation in LOX enzymes is partly controlled by an active site residue conserved as Ala in *S*-LOX and Gly in *R*-LOX (19). eLOX3 has Ala in this position. Recently, Cristea and Oliw (33) reported that mutation of the natural Gly to Ala in manganese lipoxygenase strongly augments hydroperoxide isomerase activity. Accordingly, it was of interest to examine whether changing Ala-451 to Gly in eLOX3 would produce the opposite effect, *i.e.* a switch from hydroperoxide isomerase to dioxygenase activity. Therefore, we mutated Ala-451 to Gly and incubated the mutant enzyme (0.5 μM) with arachidonic acid (42 μM). Unlike wild-type eLOX3, A451G eLOX3 reacted well with arachidonic acid even in the absence of fatty acid hydroperoxides, yet only after an unusually long lag phase of ~20 min (Fig. 3*B*). This lag phase could be eliminated by addition of 11 μM 13*S*-HPODE at the beginning of the reaction (Fig. 3*B*).

Effect of Temperature on Accumulation of HPETE Products—In the room temperature reactions mentioned above, the expected HPETE products occurred only as transient intermedi-

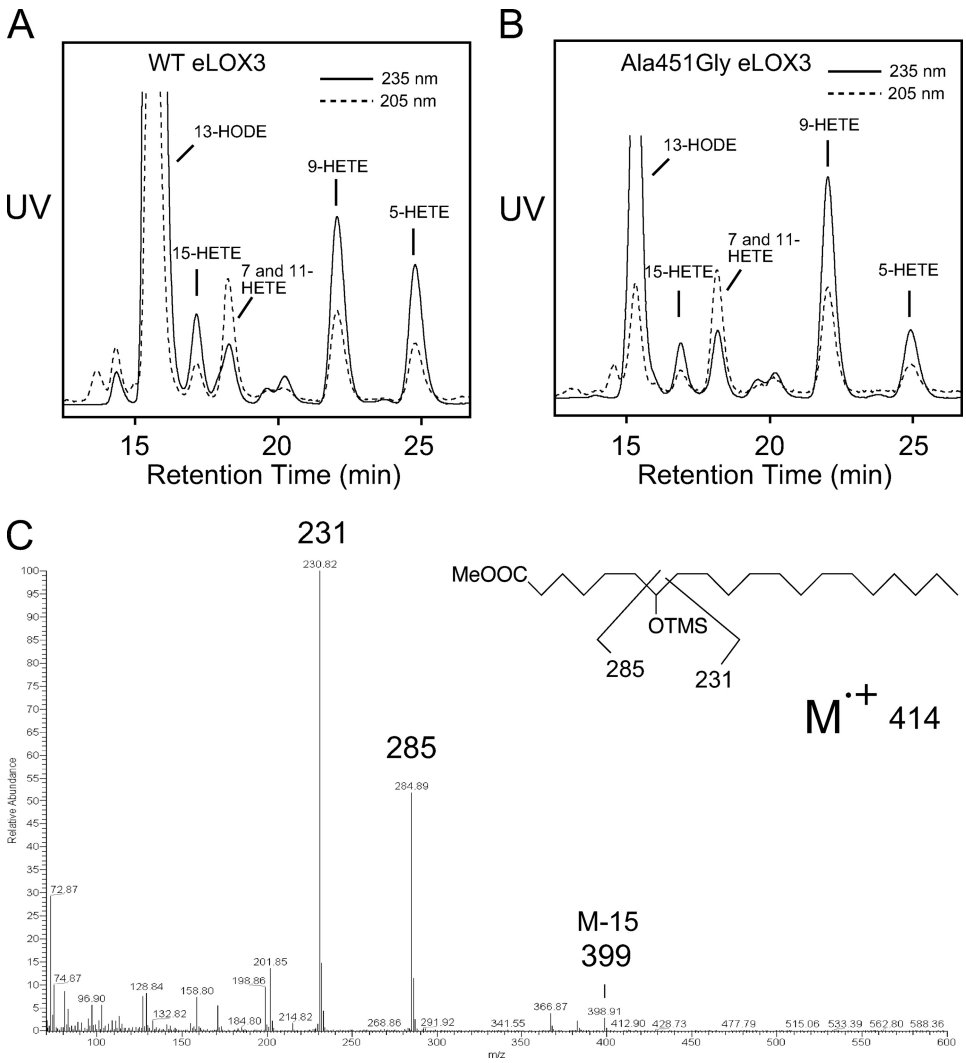

FIGURE 5. **Identification of products from reactions of wild-type eLOX3 and A451G eLOX3 with arachidonic acid.** The incubation conditions were the same as in Fig. 4, *B* and *D*. *A* and *B*, RP-HPLC analysis of products from wild-type and A451G eLOX3, respectively. *C*, GC-MS analysis of TMS ether methyl ester derivative of hydrogenated 7-HETE product. Before hydrogenation and derivatization, the 7-HETE product had been further purified by SP-HPLC.

ates with either the wild-type or A451G eLOX3 (Fig. 4, *A* and *C*); the primary hydroperoxide products are further converted to epoxyalcohols and ketones by the hydroperoxide isomerase activity of eLOX3 (data not shown). However, similar to the observations with 9*E*,11*Z*,14*Z*-20:3ω6, when reaction with arachidonic acid was performed at 0 °C and in the presence of excess 13*S*-HPODE, the HPETE products continued to accumulate during the entire course of the reaction (Fig. 4, *B* and *D*), and the epoxyalcohol and ketone secondary products were formed only in negligible amounts.

Identification of the HPETE Products—After the reaction, the HPETE products from the 0 °C incubation were reduced with $SnCl_2$, extracted using a C_{18} cartridge, and subjected to RP- and SP-HPLC analyses. As shown in Fig. 5*A*, the products consisted of predominantly 7-, 9-, and 5-H(P)ETEs (25, 29, and 22%, respectively) that stemmed from C-7 hydrogen abstraction, followed by 15- and 11-H(P)ETEs (8 and 9% respectively) from C-13 hydrogen abstraction. 12- and 8-H(P)ETEs were formed only in minor amounts (less than 3% each). The identity of the unusual bis-allylic 7-H(P)ETE product was unequivocally established by GC-MS analysis of its methyl ester TMS ether derivative, before and after catalytic hydrogenation (supplemental Fig. S3 and Fig. 5*C*).

Consistent with this lack of positional specificity, further analysis by chiral HPLC indicated no remarkable stereospecificity in any of the positional isomers (Fig. 6, *A*, *C*, and *E*). Among the three major products, 7-H(P)ETE showed the highest degree of stereospecificity, being 73% 7*R*. The 5-H(P)ETE product ranked the second, being 62% 5*R*, and the 9-H(P)ETE product was essentially racemic.

The active site Ala-Gly substitution in other LOX enzymes can lead to relatively dramatic changes in product profile (19, 22, 34) or mainly to changes in stereochemistry (35). The most noticeable effect of the A451G mutation in eLOX3 was a switch toward more 9-H(P)ETE, increased from 28.9 ± 1.4% (mean ± S.E., $n = 4$) to 38.5 ± 1.0%, seemingly at the expense of 5-H(P)ETE, decreased from 21.7 ± 0.8 to 11.6 ± 1.0% (*cf.* Fig. 5, *A* and *B*). These differences were statistically significant ($p < 0.01$). Chiral HPLC analysis further revealed that the 9-H(P)ETE in the A451G

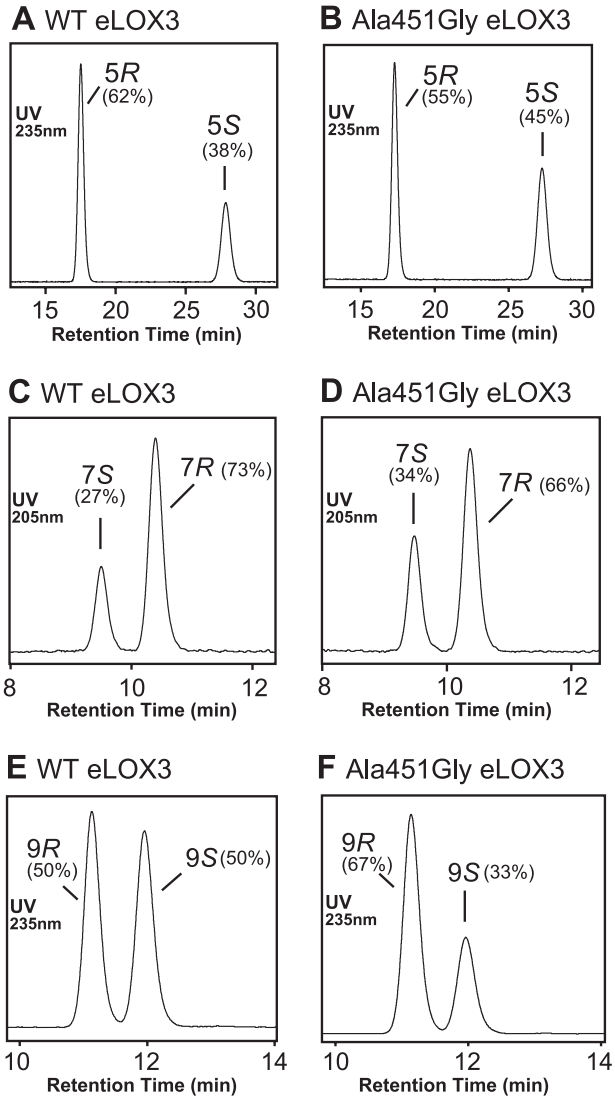

FIGURE 6. **Chiral HPLC analysis of individual HETE products from reactions of wild-type eLOX3 and A451G eLOX3 with arachidonic acid.** *A,* wild-type eLOX3, 5-HETE methyl ester. *B,* A451G eLOX3, 5-HETE methyl ester. *C,* wild-type eLOX3, 7-HETE methyl ester. *D,* A451G eLOX3, 7-HETE methyl ester. *E,* wild-type eLOX3, 9-HETE methyl ester. *F,* A451G eLOX3, 9-HETE methyl ester.

eLOX3 reaction was 67% 9*R* (Fig. 6*F*), an improvement in stereospecificity compared with the racemic 9-H(P)ETE product of wild-type eLOX3 (Fig. 6*E*).

Dioxygenase Activity of eLOX3 with AA/Lyso-PA—Experiments using AA/lyso-PA as substrate, a molecule with a bulky ester on the arachidonate carboxyl, were used to gain insight into the possible "tail first" or "head first" substrate binding orientation (36, 37). Reaction occurred at less than 0.1% of the rate with free arachidonic acid, and products arising mainly from C-13 hydrogen abstraction were formed (supplemental Fig. S4). These results strongly suggest that the tail first orientation of substrate binding is mainly associated with H-13 abstraction in the reaction of wild-type or A451G eLOX3 with AA/lyso-PA. It can be further inferred that the head first orientation is associated with H-7 abstraction and is the preferred orientation in the reaction of eLOX3 with free arachidonic acid.

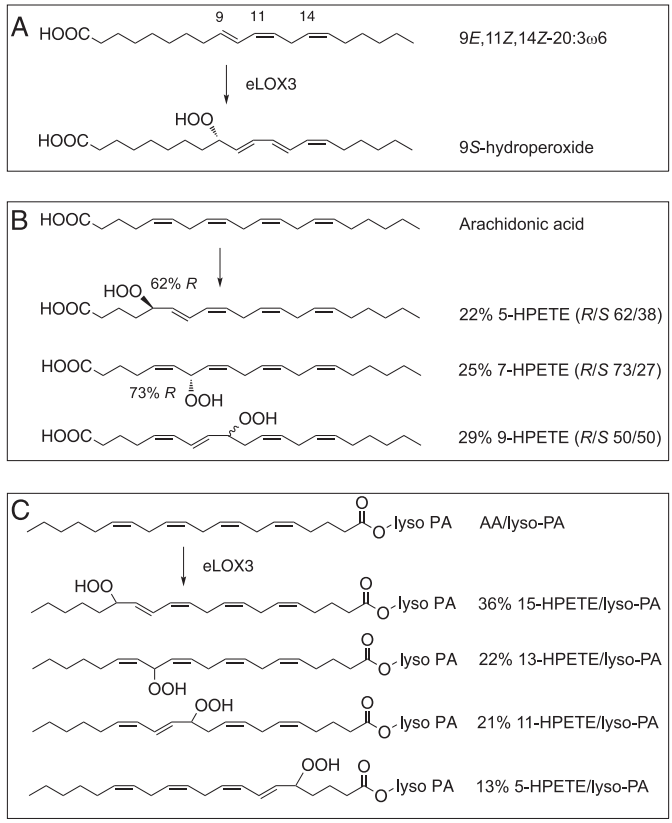

FIGURE 7. **Dioxygenase activity of eLOX3.**

DISCUSSION

Discovery of Dioxygenase Activity in eLOX3

This study demonstrates that eLOX3 in its active form is capable of oxygenating polyunsaturated fatty acids to the fatty acid hydroperoxides. As summarized in Fig. 7, eLOX3 oxygenates 9*E*,11*Z*,14*Z*-20:3ω6 in a regio- and stereospecific fashion to give the 9*S*-hydroperoxide. Although the reaction with arachidonic acid is much slower and exhibits considerably less specificity (Fig. 7), the enzymatic nature of this reaction is confirmed by the formation of 7-HPETE, which cannot be formed nonenzymatically under the conditions used in this study. Such bis-allylic hydroperoxides are formed from the corresponding peroxyl radical only in the presence of a highly efficient hydrogen atom donor (38, 39), which in this case is not present in the incubation buffer and thus must be part of the enzyme machinery, most likely the Fe(II)-H_2O complex. eLOX3 joins manganese lipoxygenase (40) and the recently characterized mini-LOX from cyanobacterium *Cyanothece* sp. (41) in the ability to make a bis-allylic hydroperoxide.

Unusual Aspects of eLOX3 and Reasons for Its Elusive Dioxygenase Activity

Our study also reveals aspects of eLOX3 that may explain why its dioxygenase activity has remained undetected for years. (i) With fatty acid substrate alone, the reaction shows an unusually long lag phase. This ranged from 4 to 5 min with 9*E*,11*Z*,14*Z*-20:3ω6 (Fig. 2*B*) to over 1 h with arachidonic acid (Fig. 3*A*). (ii) Compared with typical LOX reactions, high concentrations of fatty acid hydroperoxide are required to abolish

the lag phase. (iii) As known with other LOX enzymes (42–44), not every fatty acid hydroperoxide is equally effective in the enzyme activation. The best substrate for the hydroperoxide isomerase activity of eLOX3, 12*R*-HPETE, turns out to be only marginally effective. This is not a coincidence, as 12*R*-HPETE allows for efficient hydroperoxide isomerase cycling of eLOX3. (iv) At room temperature (as opposed to at 0 °C), the primary oxygenation products occur only as transient intermediates, *i.e.* they will be further converted to epoxyalcohols and ketones by the hydroperoxide isomerase activity. Therefore, the reaction gives no signal with the usual spectrophotometric (UV 235 nm) or HPLC-UV assays.

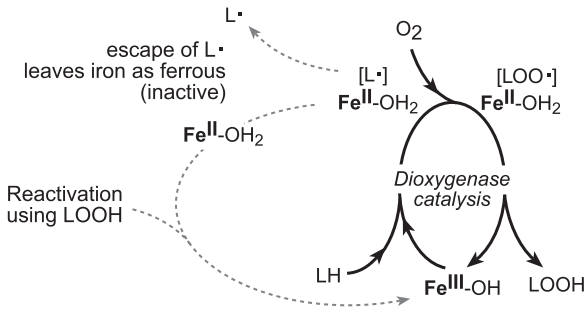

FIGURE 8. **LOX catalytic cycle.** *Solid lines,* when oxygen access is not limited; *dotted lines,* when oxygen access is limited.

Our Interpretations of the Unusual Aspects

The evidence points to a deficiency in the activation of eLOX3. Whereas 1 eq of fatty acid hydroperoxide activator is sufficient in the activation step of typical LOX, many equivalents are required in the activation step of eLOX3, hence the pronounced lag phase and the requirement for high concentrations of a fatty acid hydroperoxide activator.

The deficiency in the activation step of eLOX3 is somewhat relieved by the A451G mutation. A451G eLOX3 appears to stand at the midpoint between wild-type eLOX3 and typical LOX. On the one hand, A451G eLOX3 still shows a pronounced lag phase in its reactions with arachidonic acid in the absence of fatty acid hydroperoxides. On the other hand, the lag phase of A451G eLOX3 is much shorter than that of wild-type eLOX3 and can be eventually overcome by only trace amounts of fatty acid hydroperoxide present in the substrate preparation.

Explaining the Difference between eLOX3 and Typical LOX

When the hydroperoxide isomerase activity of eLOX3 was originally characterized, our group had speculated that the enzyme fails to oxygenate natural fatty acids because the active site iron has a lower redox potential than the iron in typical LOX (10). As already outlined in the Introduction, hydrogen abstraction on typical fatty acid substrates, which is the first step of LOX catalysis, calls for a moderately high redox potential, and conceivably the redox potential could be exceptionally low in eLOX3 due to some unfavorable protein environment of the enzyme active site. However, this is not immediately evident on inspection of the protein sequence, as all the typical conserved features of LOX enzymes, including the conserved amino acid ligands to the iron, are retained in eLOX3. Most importantly, this issue is now addressed as we have demonstrated in this study that arachidonic acid can be oxidized by eLOX3 (with H-7 preferentially abstracted by the iron complex), thus definitively ruling out this low redox potential possibility.

To account for the atypical dioxygenase activity of eLOX3, we invoke an alternative explanation, that oxygen access is limited in the enzyme active site. Because molecular oxygen is one of the two substrates in LOX catalysis, limited oxygen access to the reacting fatty acid radical intermediate would undoubtedly impede catalysis. In the extreme scenario, when molecular oxygen is not available at all either because oxygen access is completely blocked or because the atmosphere is rendered anaerobic, even though the initial C–H bond cleavage step may proceed normally, the fatty acid radical thus produced would eventually escape from the enzyme active site in the absence of reacting molecular oxygen, leaving the enzyme in the inactive ferrous state (Fig. 8). Such a single turnover event would be undetectable in typical enzyme assays. Under such circumstances, redox cycling can occur only if the ferrous enzyme is re-oxidized by hydroperoxide back to the ferric form (Fig. 8, *dotted line*), as seen classically in the anaerobic reaction of soybean LOX with linoleic acid and 13*S*-HPODE (45, 46). However, under the usual aerobic conditions, such an extreme scenario hardly applies to typical LOX, indicating that molecular oxygen is readily accessible to the reacting fatty acid radical in their active site. For example, it is estimated that free radical leakage occurs only once per hundred turnovers in the reaction of soybean LOX-1 with linoleic acid (13). We suggest that limited oxygen access is the actual case in eLOX3, based on the following interpretations of the following evidence.

Carbon Radicals Escape from the Active Site during Dioxygenase Cycling—In the transformation of arachidonic acid at room temperature, the hydroperoxide isomerase activity is persistent throughout the reaction, and HPETE products fail to accumulate (*cf.* Fig. 4, *A* and *C*), indicating that the ferrous enzyme is constantly produced. Also, the reaction of eLOX3 with arachidonic acid is clearly driven by 13*S*-HPODE (Fig. 3*A*, the curve with two doses of 13*S*-HPODE), just as the anaerobic conversion of linoleic acid by soybean LOX-1 is driven by 13*S*-HPODE. These observations can be explained if a significant portion of fatty acid carbon radical intermediates escapes from the active site, which could be the result of lack of reacting oxygen (*cf.* Fig. 8). Although leakage of peroxyl radical instead of carbon radical is also conceptually plausible, we consider this rather unlikely, because the subsequent trapping of peroxyl radical by the enzyme is remarkably efficient as indicated by formation of the bis-allylic product, 7-HPETE.

Lack of Regio- and Stereo-specificity within the Active Site—The lack of oxygenation specificity with arachidonic acid is not entirely due to radical leakage and subsequent nonenzymatic oxygenation in solution. This is indicated by the appearance of 7-HPETE, which must be generated entirely within the enzyme active site. The *R*/*S* ratio of 73:27 in 7-HPETE must reflect a combination of the differences in oxygen supply to the two faces of C-7 and in trapping effi-

ciency of the respective 7*R*- and 7*S*-peroxyl radicals. Indeed, it is likely that oxygen is added nonselectively to every reacting site on the delocalized pentadienyl radical (*e.g.* C-5, C-7, and C-9 when H-7 is abstracted), suggesting that oxygen supply is similarly low in every reacting site.

A451G Mutation Augments Dioxygenase Activity—A451G eLOX3 shows "improved" specificity in its reaction with arachidonic acid compared with wild-type eLOX3, in that both the proportion of 9-HPETE among all isomers and its *R*/*S* ratio increase considerably. We deduce that the Ala-to-Gly mutation opens up space and introduces an oxygen "pocket" that is aligned with the "9*R*" site on arachidonic acid.

eLOX3 Readily Oxygenates 9E,11Z,14Z-20:3ω6—This synthetic fatty acid with extended conjugation is a much better substrate than arachidonic acid and is oxygenated regio- and stereospecifically to the 13*S*-hydroperoxide. This is consistent with the availability of an oxygen pocket in this unusual 9*S* position, which is four carbons removed from the site of hydrogen abstraction at C-13. Obviously, such a pocket or channel would play no role in the oxygenation of typical pentadienyl fatty acids that require oxygen to be delivered to sites that are two carbons removed from the site of hydrogen abstraction.

Connection between Oxygen Access and Enzyme Activation

The natural question at this point is how our proposed difference of eLOX3 from typical LOX, *i.e.* limited oxygen access, would lead to a deficiency in the enzyme activation step. A kinetic study of rabbit reticulocyte 15-LOX-1 suggests that molecular oxygen is in fact directly involved in the LOX activation step (47). We have evidence from comparison of soybean LOX-1 and eLOX3 that agrees with this proposition and further suggests that molecular oxygen is actually a driving force in the activation step (52). Therefore, it is not surprising that the activation step would be impaired when oxygen access in the active site becomes limited.

Concluding Remarks

In this study we have unveiled dioxygenase activity of eLOX3 with fatty acids and investigated both the usual and unusual aspects. The usual aspects suggest that the basic machinery for LOX catalysis is fully functional in eLOX3, whereas the unusual aspects of eLOX3 point to the possibility that eLOX3 has limited oxygen access in the active site. It may be useful to consider a spectrum of activities among LOX enzymes that are partly dependent on the availability of molecular oxygen within the respective enzyme active sites. At one end of the spectrum are the conventional LOX, exemplified by soybean LOX-1, in which dioxygenase activity is dominant. Toward the other end of the spectrum, with limited access to molecular oxygen and radical leakage from the active sites, are atypical LOX enzymes such as eLOX3, plant type-2 lipoxygenases (48, 49), moss and maize LOX with hydroperoxide isomerase, and lyase activities (50, 51).

As noted at the beginning of the Introduction, eLOX3 performs a vital function in epidermal barrier formation. Where do our new findings stand in relation to this physiological role, and what is their importance? When the hydroperoxide isomerase activity of eLOX3 was discovered originally, it was presumed that this atypical isomerase activity, acting on a hydroperoxide product of its partner 12*R*-LOX, represents the function of eLOX3 *in vivo*. As the evidence stands at present, we continue to favor this interpretation, although whether this dioxygenase activity in eLOX3 is physiologically relevant should be considered in future studies. In our view, the latent dioxygenase activity of eLOX3 is a reflection of mechanistic issues biasing eLOX3 toward hydroperoxide isomerase activity.

Acknowledgment—We thank William E. Boeglin for help with expression and purification of eLOX3.

REFERENCES

1. Brash, A. R., Yu, Z., Boeglin, W. E., and Schneider, C. (2007) *FEBS J.* **274,** 3494–3502
2. Fürstenberger, G., Epp, N., Eckl, K. M., Hennies, H. C., Jørgensen, C., Hallenborg, P., Kristiansen, K., and Krieg, P. (2007) *Prostaglandins Other Lipid Mediat.* **82,** 128–134
3. Fischer, J. (2009) *J. Invest. Dermatol.* **129,** 1319–1321
4. Jobard, F., Lefèvre, C., Karaduman, A., Blanchet-Bardon, C., Emre, S., Weissenbach, J., Ozgüc, M., Lathrop, M., Prud'homme, J. F., and Fischer, J. (2002) *Hum. Mol. Genet.* **11,** 107–113
5. Elias, P. M., Williams, M. L., Holleran, W. M., Jiang, Y. J., and Schmuth, M. (2008) *J. Lipid Res.* **49,** 697–714
6. Epp, N., Fürstenberger, G., Müller, K., de Juanes, S., Leitges, M., Hausser, I., Thieme, F., Liebisch, G., Schmitz, G., and Krieg, P. (2007) *J. Cell Biol.* **177,** 173–182
7. Krieg, P., de Juanes, S., Epp, N., Rosenberger, S., Furstenberger, G., Hausser, I., Thieme, F., Liebisch, G., Schmitz, G., and Stark, H. (2010) *The 12th International Winter Eicosanoid Conference, March 7–10, 2010,* Baltimore, MD
8. Moran, J. L., Qiu, H., Turbe-Doan, A., Yun, Y., Boeglin, W. E., Brash, A. R., and Beier, D. R. (2007) *J. Invest Dermatol.* **127,** 1893–1897
9. Kinzig, A., Heidt, M., Fürstenberger, G., Marks, F., and Krieg, P. (1999) *Genomics* **58,** 158–164
10. Yu, Z., Schneider, C., Boeglin, W. E., Marnett, L. J., and Brash, A. R. (2003) *Proc. Natl. Acad. Sci. U.S.A.* **100,** 9162–9167
11. Schilstra, M. J., Veldink, G. A., and Vliegenthart, J. F. G. (1994) *Biochemistry* **33,** 3974–3979
12. Haining, J. L., and Axelrod, B. (1958) *J. Biol. Chem.* **232,** 193–202
13. Schilstra, M. J., Veldink, G. A., and Vliegenthart, J. F. G. (1993) *Biochemistry* **32,** 7686–7691
14. Kemal, C., Louis-Flamberg, P., Krupinski-Olsen, R., and Shorter, A. L. (1987) *Biochemistry* **26,** 7064–7072
15. Glickman, M. H., and Klinman, J. P. (1996) *Biochemistry* **35,** 12882–12892
16. Pratt, D. A., Mills, J. H., and Porter, N. A. (2003) *J. Am. Chem. Soc.* **125,** 5801–5810
17. Que, L., Jr., and Ho, R. Y. (1996) *Chem. Rev.* **96,** 2607–2624
18. Nelson, M. J. (1988) *Biochemistry* **27,** 4273–4278
19. Coffa, G., and Brash, A. R. (2004) *Proc. Natl. Acad. Sci. U.S.A.* **101,** 15579–15584
20. Coffa, G., Schneider, C., and Brash, A. R. (2005) *Biochem. Biophys. Res. Commun.* **338,** 87–92
21. Brash, A. R., and Song, W. (1996) *Methods Enzymol.* **272,** 250–259
22. Zheng, Y., Boeglin, W. E., Schneider, C., and Brash, A. R. (2008) *J. Biol. Chem.* **283,** 5138–5147
23. Nugteren, D. H., and Christ-Hazelhof, E. (1987) *Prostaglandins* **33,** 403–417
24. Boutaud, O., and Brash, A. R. (1999) *J. Biol. Chem.* **274,** 33764–33770
25. Huang, L. S., Kim, M. R., and Sok, D. E. (2006) *Arch. Biochem. Biophys.* **455,** 119–126
26. Brash, A. R., Boeglin, W. E., Capdevila, J. H., Yeola, S., and Blair, I. A.

(1995) *Arch. Biochem. Biophys.* **321,** 485–492
27. Brash, A. R., Ingram, C. D., and Harris, T. M. (1987) *Biochemistry* **26,** 5465–5471
28. Brash, A. R., Yokoyama, C., Oates, J. A., and Yamamoto, S. (1989) *Arch. Biochem. Biophys.* **273,** 414–422
29. Clapp, C. H., Strulson, M., Rodriguez, P. C., Lo, R., and Novak, M. J. (2006) *Biochemistry* **45,** 15884–15892
30. Pistorius, E. (1974) *Studies on Isoenzymes of Soybean Lipoxygenase*, Ph.D. thesis, Purdue University
31. Salzmann, U., Kühn, H., Schewe, T., and Rapoport, S. M. (1984) *Biochim. Biophys. Acta* **795,** 535–542
32. Butovich, I. A., and Reddy, C. C. (2001) *Biochim. Biophys. Acta* **1546,** 379–398
33. Cristea, M., and Oliw, E. H. (2006) *J. Biol. Chem.* **281,** 17612–17623
34. Andreou, A. Z., Vanko, M., Bezakova, L., and Feussner, I. (2008) *Phytochemistry* **69,** 1832–1837
35. Meruvu, S., Walther, M., Ivanov, I., Hammarström, S., Fürstenberger, G., Krieg, P., Reddanna, P., and Kuhn, H. (2005) *J. Biol. Chem.* **280,** 36633–36641
36. Kuhn, H., Saam, J., Eibach, S., Holzhütter, H. G., Ivanov, I., and Walther, M. (2005) *Biochem. Biophys. Res. Commun.* **338,** 93–101
37. Schneider, C., Pratt, D. A., Porter, N. A., and Brash, A. R. (2007) *Chem. Biol.* **14,** 473–488
38. Brash, A. R. (2000) *Lipids* **35,** 947–952
39. Tallman, K. A., Pratt, D. A., and Porter, N. A. (2001) *J. Am. Chem. Soc.* **123,** 11827–11828
40. Su, C., and Oliw, E. H. (1998) *J. Biol. Chem.* **273,** 13072–13079
41. Andreou, A., Göbel, C., Hamberg, M., and Feussner, I. (2010) *J. Biol. Chem.* **285,** 14178–14186
42. Cristea, M., and Oliw, E. H. (2007) *J. Lipid Res.* **48,** 890–903
43. Kühn, H., Wiesner, R., Stender, H., Schewe, T., Lankin, V. Z., Nekrasov, A., and Rapoport, S. M. (1986) *FEBS Lett.* **203,** 247–252
44. Pérez-Gilabert, M., Sánchez-Felipe, I., Morte, A., and García-Carmona, F. (2005) *J. Agric. Food Chem.* **53,** 6140–6145
45. de Groot, J. J., Veldink, G. A., Vliegenthart, J. F. G., Boldingh, J., Wever, R., and van Gelder, B. F. (1975) *Biochim. Biophys. Acta* **377,** 71–79
46. Garssen, G. J., Vliegenthart, J. F. G., and Boldingh, J. (1971) *Biochem. J.* **122,** 327–332
47. Ivanov, I., Saam, J., Kuhn, H., and Holzhütter, H. G. (2005) *FEBS J.* **272,** 2523–2535
48. Axelrod, B., Cheesbrough, T. M., and Laakso, S. (1981) *Methods Enzymol.* **71,** 441–451
49. Fukushige, H., Wang, C., Simpson, T. D., Gardner, H. W., and Hildebrand, D. F. (2005) *J. Agric. Food Chem.* **53,** 5691–5694
50. Gao, X., Stumpe, M., Feussner, I., and Kolomiets, M. (2008) *Planta* **227,** 491–503
51. Senger, T., Wichard, T., Kunze, S., Göbel, C., Lerchl, J., Pohnert, G., and Feussner, I. (2005) *J. Biol. Chem.* **280,** 7588–7596
52. Zheng, Y., and Brash, A. R. (2010) *J. Biol. Chem.* **285,** 39876–39887